

# Flux smelting behavior of pre-reduced Mn ore by Hydrogen at elevated temperatures

*Pankaj Kumar<sup>1</sup> and Jafar Safarian<sup>2</sup>*

1. PhD candidate, Department of Materials Science and Engineering, NTNU  
N-7034 Trondheim, Norway. Email: Pankaj.kumar@ntnu.no
2. Professor, Department of Materials Science and Engineering, NTNU  
N-7034 Trondheim, Norway. Email: jafar.safarian@ntnu.no

Keywords: smelting, hydrogen reduction, sessile drop test, slag, iron, manganese, flux, lime.

## ABSTRACT

Understanding how ore interacts with flux particles at elevated temperatures to create molten slag is crucial since it governs the dynamics of a chemical reaction. This study explores the smelting behaviour of pre-reduced Nchwanning manganese ore when combined with lime, with the objective of examining the evolving interaction between pre-reduced ore particles and lime over time. The research sheds light on the interaction between solid and liquid and the phases that emerge during this process. To achieve this, a sessile drop furnace was employed to rapidly heat the materials positioned adjacent to each other on an alumina substrate and to observe the smelting process as it unfolded over time. This method allowed for the direct observation of the melting temperatures and the flux-ore reaction progression rate, and the potential disruptive events that might occur. By comparing the molten interfaces of the fluxed materials at various time intervals, this study provides insights into the relative rate of slag formation from the two materials. The results indicate that the main slag formation initiated at approximately 1400 °C and continued to advance with time, with complete mixing occurring around 1500 °C. The possible phases formed were identified using Scanning Electron Microscopy and modelled using Fact Sage thermodynamic software. In addition, the iron particles in the pre-reduced Mn ore were separated and settled from a rich MnO-containing slag. It was found that the separation of molten iron droplets from the slag depends on the rate of solid MnO particles dissolution into the adjacent slag phase.

## 1. INTRODUCTION

Ferromanganese production consumes anywhere between 2400-2700 kWh energy per ton of metal produced [1]. Ferroalloys such as ferromanganese are mainly produced in submerged arc furnaces [2], where 50-70 % of the required thermal energy is given by electrical dissipation and the rest is met by carbon or other carbonaceous material like biomass and charcoal [3], which is used as a reductant. The process of manganese production goes through series of reduction steps as shown in eq.1-3 [1]. Where the higher manganese oxide is reduced to lower oxide by indirect reduction by CO gas followed by final step where the manganese monoxide is reduced to manganese metal by carbon eq. 4 [1].



The process emits huge amount of greenhouse gas (GHG) which greatly depends on the source of energy and reductant material (biomass, metallurgical coke, or coal [4], [5]. It was found from the previous studies that around 1.04 to 6.0 kg CO<sub>2</sub> is emitted per kg FeMn production [4]–[6]. The CO<sub>2</sub>

is responsible for 20 % of thermal absorption, which directly causes global warming [7] and climate change, which is recognized as a substantial threat to human health [8], [9]. With more awareness and stricter government rules, industries are forced to move towards greener alternative routes to produce these metal and alloys. One such route is the use of hydrogen, for the reduction of metal oxides like  $\text{Cr}_2\text{O}_3$  [10],  $\text{Fe}_2\text{O}_3$  [11],  $\text{MnO}_2$  [12], [13], to its lower oxides. The use of hydrogen produces water vapor as the main off-gas component which is safe and even can be further used, hence significantly reducing  $\text{CO}_2$  emission. Manganese oxide can only be partially reduced with hydrogen following eq. 5-7, [13] unlike iron oxide that can be completely reduced with hydrogen following eq. 8.



The pre-reduction of manganese ore with hydrogen significantly reduces the net  $\text{CO}_2$  emission from the process. In a recent approach, of which this manuscript is a part of, researchers have tried coupling the use of hydrogen for pre-reduction of manganese ore followed by aluminium for complete reduction of the pre-reduced ore following eq. 9. the process is referred to as HAlMan [13].



The reaction being highly exothermic in nature gives enough energy for slag metal formation and separation. The slag formed in the process mostly contains  $\text{Al}_2\text{O}_3$ ,  $\text{CaO}$  and some unreduced  $\text{MnO}$  along with low amount of  $\text{SiO}_2$  and  $\text{MgO}$ . One of the major aims in the HAlMan process is to generate slag which could be leached to recover alumina and calcia. The recovered alumina and calica can be re-used in the process, hence further reducing the net energy consumption. But, for this to be achieved, the slag needs to be designed well to be easily leachable. It is found from the literature that calcium aluminat ( $\text{CaAl}_2\text{O}_4$ ) phase is the most easily leached phase [14], while gehlenite phase ( $\text{Ca}_2\text{Al}_2\text{SiO}_7$ ) is tough to be leached.

To achieve the required phase, it is of prime importance to understand the mechanisms of phases formation and transformation with time and temperature. The current manuscript focuses on studying the interaction of flux ( $\text{CaO}$ ) with a pre-reduced Mn ore by  $\text{H}_2$  gas on alumina. The study is performed in a sessile drop test furnace, where the lime and pre-reduced ore particles are placed on the alumina substrate and heated at various rates and durations to monitor softening, melting and interaction of material upon heating. After the tests, the microstructure and composition of samples are studied by microscopic examination.

## 2. EXPERIMENTAL

### 2.1. Method

The overall experimental procedure of this work is presented in Fig. 1. The detail about the experiment is provided in later sections.

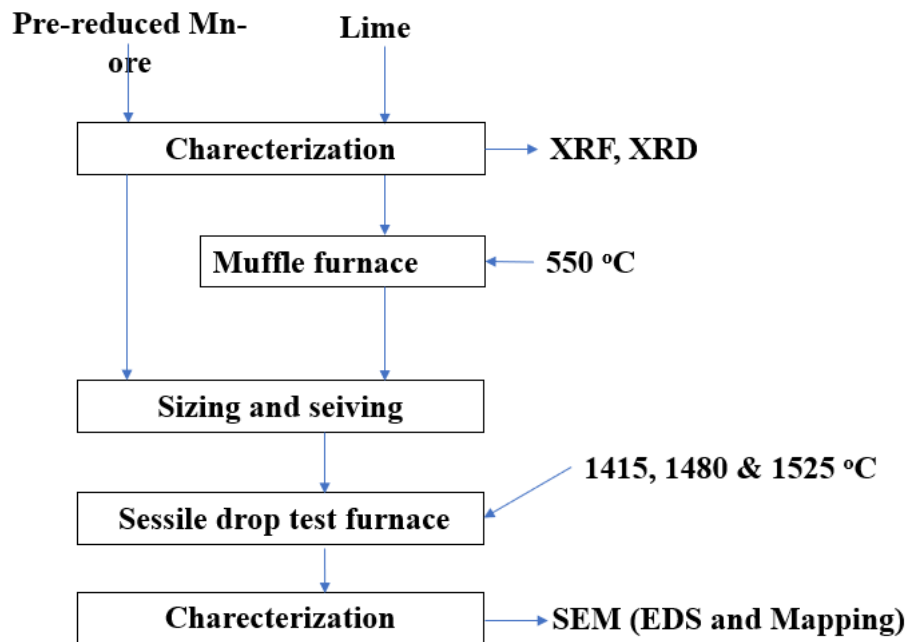
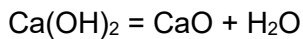


Figure 1: Schematic of used methodology showing the materials flow.

## 2.2. Materials and Preparation

A pre-reduced Nchwani ore and lime was used for the study. The pre-reduction of the Nchwani ore was carried out using a vertical tube resistance furnace, which is designed to reach a maximum temperature of 1100 °C and can purge Ar, H<sub>2</sub> and CO gas. 50 g of dried Nchwani ore in the size range of 4-10 mm was reduced with hydrogen at a flow rate of 4Nl/min, held at 800 °C for 1 hour. The reduced sample was then crushed and sieved to obtain particles of size 2-3 mm, which was then sealed in an airtight plastic bag to prevent any reoxidation. Similarly, the lime was pre-heated to 550 °C under Ar atmosphere, to decompose any calcium hydroxide formed due to exposure to atmosphere for long time. Following the reaction in eq 10.



$$\Delta H_{298}^{\circ} = 104.903 \text{ kJ/mol} \quad (10)$$

After pre-heating, the lime samples were collected and sealed in airtight plastic to avoid hydration. The lime particles were carefully sized to 2-3 mm manually, as they are quite soft and may turn fine on pulverizing mechanically. These sized particles were then kept for further sessile drop test study.

## 2.3. Sessile Drop test.

Particles of similar size, from the size range of 2-3 mm were taken from each pre-reduced Nchwani ore and lime. One particle each of pre-reduced Nchwani ore and lime was kept on alumina substrate, which was then kept on the graphite holder Fig.2. The sample holder was then pushed inside the furnace sealed, evacuated, and backfilled to atmospheric pressure with argon. The argon flow of 0.5 Nl/min was maintained throughout the test. For all the test similar schedule was used. The schedule comprised of four stages shown in Table 1. Starting of the interaction of lime and pre-reduced ore particle and the completion of melting of the samples were made the two end points of the experiment, and an intermediate stage between them was also considered for study. It was observed that the interaction started at 1415 °C, and was completed at 1525 °C, these two points were considered as the two end points and designated as T1 and T3, respectively, while the intermediate temperature 1480 °C will be marked as T2 for ease of discussion.

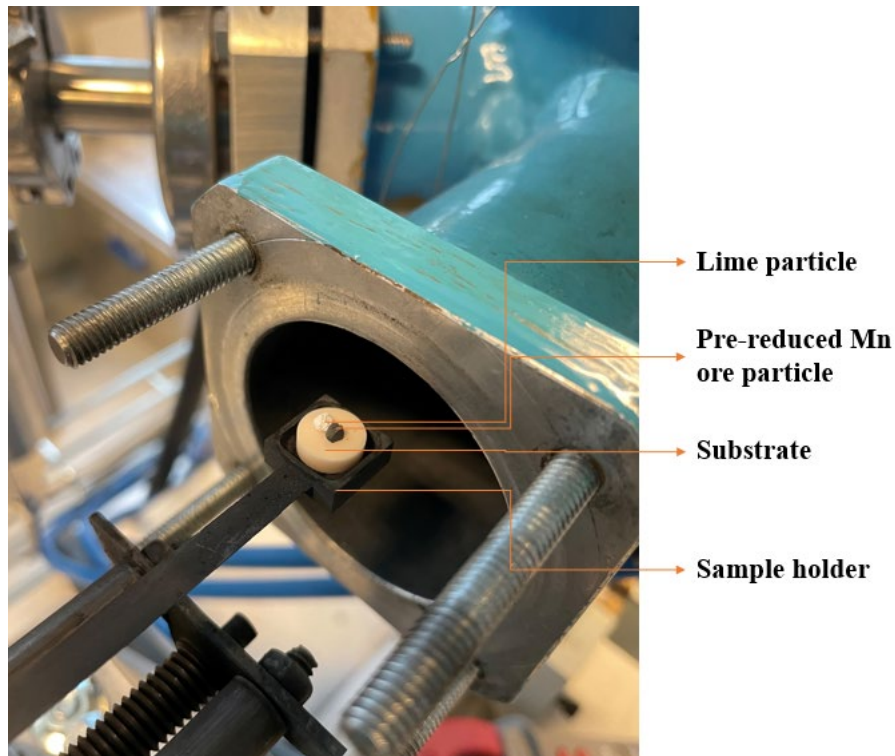


Figure 2: Samples placed on Sample holder.

Table 1: Program for sessile drop test furnace

Total time [HH:MM:SS]	Time interval [HH:MM:SS]	End temp. (°C)	Ar flow rate (NI/min)
00:00:30	00:00:30	25	0.5
00:03:30	00:03:00	900	0.5
00:09:30	00:06:00	1200	0.5
00:49:30	00:40:00	1800	0.5
00:59:30	00:10:00	25	0.5

Figure 3 depicts the schematic of the sessile drop test furnace comprising three key components: the primary heating chamber equipped with heating element and a thermocouple, a firewire digital video camera with a telecentric zoom Lense capable of capturing images at 1280×960 pixels resolution situated to the right, and a pyrometer on the left for temperature measurement. The furnace offers a capability to purge CO, hydrogen, and inert gas, facilitating the examination of pre-reduction behaviour or properties such as melting point and surface tension. In this specific instance, the focus was solely on understanding the smelting characteristic of the pre-reduced Nchwani manganese ore with lime particle and alumina substrate.

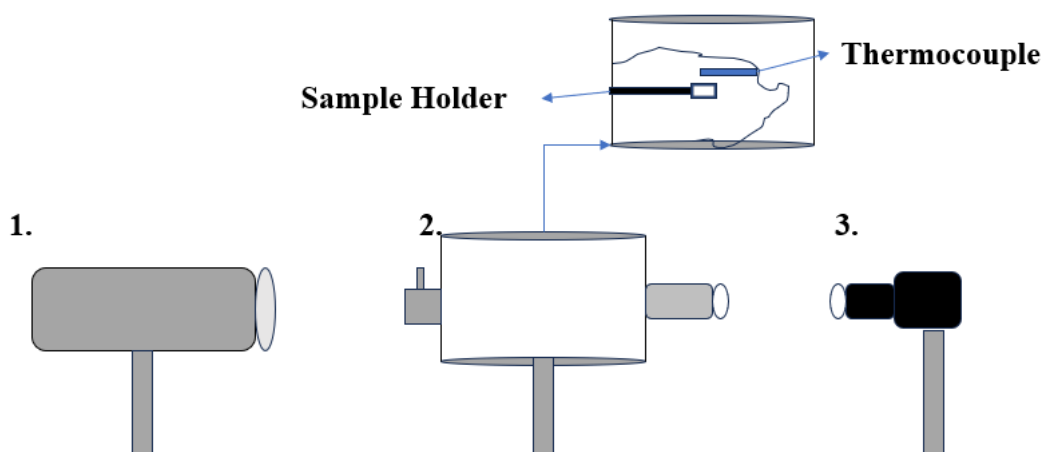


Figure 3: Schematic of Sessile drop test furnace wherein 1. represents the pyrometer, 2. main chamber and 3. the Camera.

### 2.3. Characterization Technique.

The pre-reduced Nchwanning ore and lime were powdered (<75  $\mu\text{m}$ ) in a ring mill for 1 min at a speed of 800 revolution per minute (rpm) and sent for elemental analysis. Elemental analysis was done using the X-ray fluorescence (XRF) technique (Thermo fisher, Degerfors laboratorium AB, Sweden). The mineralogical examination through X-ray diffraction (XRD) was done using the Bruker D8 A25 DaVinci™ equipment from Karlsruhe, Germany. For lime samples the XRD analysis was carried out both before and after pre-heating to be sure about complete decomposition of  $\text{Ca}(\text{OH})_2$  to  $\text{CaO}$ . The XRD for each sample was done for  $2\theta$  ranging from 0-80 degrees, with a step size of  $0.2^\circ$ . The diffraction analysis of the phases was conducted using a crystallographic database and EVA software. The samples after sessile drop test were cold mounted using epoxy and polished using automatic polishing machine Tegrapol 30. The polished sample was observed under scanning electron microscope (SEM) (Zeiss ultra 55LE, Carl Zeiss, Jena, Germany) for microstructural analysis using. While the elemental analysis and mapping was done using energy dispersive spectroscopy (EDS) (Bruker, AXS, microanalysis GmbH, Berlin, Germany).

The chemical composition of pre-reduced Nchwanning ore and lime is presented in Table 2. A major fraction of the weight of pre-reduced ore is composed of manganese monoxide and reduced iron. Limestone mostly contains  $\text{CaO}$  and small amount of  $\text{MgO}$  and  $\text{SiO}_2$ .

Table 2: XRF elemental analysis of pre-reduced Nchwanning ore and lime sample (wt%).

Sample	%MnO	%Fe	% $\text{Al}_2\text{O}_3$	% $\text{SiO}_2$	%CaO	%MgO	%LOI
Lime	-	-	0.16	0.19	90.20	0.50	8.45
Pre-reduced Nchwanning ore	72.22**	12.21*	0.43	4.66	8.93	1.48	-

\*metallic iron, \*\*in form of MnO

## 3. RESULTS AND DISCUSSION

### 3.1. Melting behaviour

The lime and the pre-reduced manganese ore particle were kept on the alumina substrate and heated. It was observed that the lime particle started melting first, at around  $1350^\circ\text{C}$  near the contact point with alumina substrate. Fig. 4 shows different stages of melting of lime particle and pre-reduced

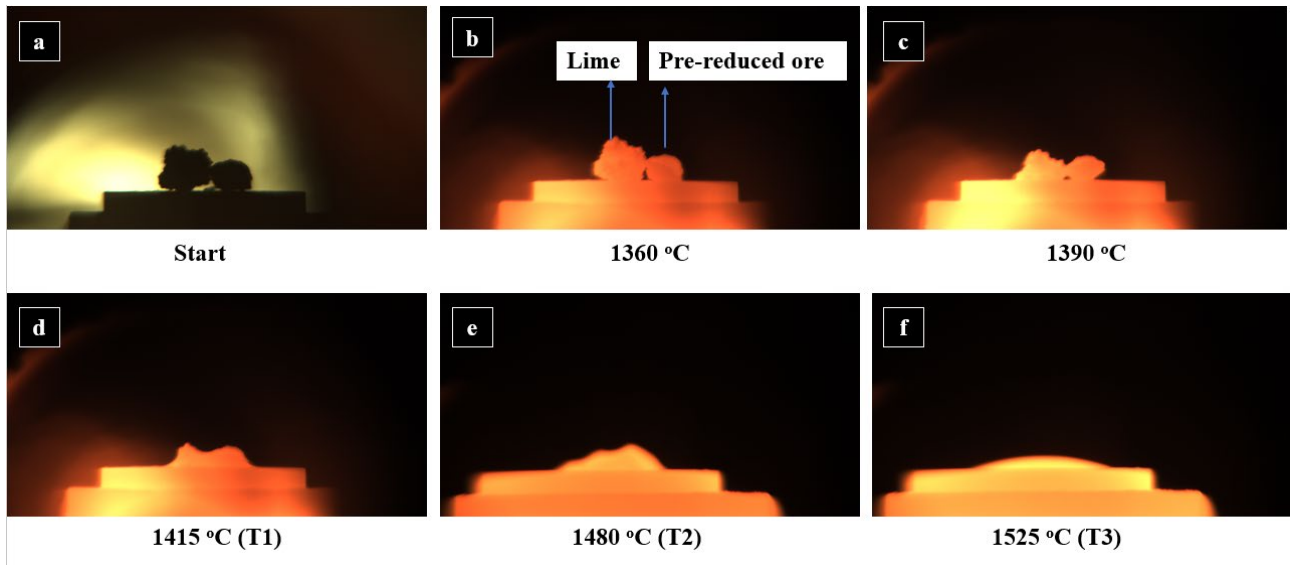


Figure 4: Different stages of interaction between lime and pre-reduced ore particle.

The interaction of molten lime particle was observed to start at around 1415 oC, while the complete melting occurred at around 1525 oC Figure 4f, where a single molten pool was observed. To further understand the interaction of lime and ore particle, microscopic examination was done which is discussed in later section.

### 3.2. Microstructural Analysis.

Figure 5 shows the microstructure of test samples for test T2. From the microstructural images three distinct region were found in samples with lower holding time and temperature (T1 & T2), which was analysed further using EDS and mapping Figure 6. The outer most region (transformed) starting from the pre-reduced manganese ore particle, was mostly observed to be composed of (37-39 wt.%) calcia and (55-57wt.%) alumina with very little (3-5 wt.%) MnO. The middle region (partially transformed) was found to contain dendritic structure, made up of the ore particle, which shows small amount of undissolved ore particle in this region. While the inner portion (un-transformed) was found to contain larger circular undissolved ore particles. The width of the middle region (partially transformed region) was observed to decrease with increasing holding time and temperature. The width in case of samples heated till 1410 oC was found to be around 250 mm which decreased to around 180 mm in case of sample heated till 1450 oC and it completely vanished for the samples heated till 1500 oC, Figure 6. The observation is obvious as the transformation is time and temperature dependent phenomenon. The reduced iron particles were mostly observed in the inner region, though there were few iron ore particles which was found suspending in the middle region. While no iron particles were observed in the outer region, the slag is already formed Figure 7. It is interesting to note that the iron particles were only observed attached to the manganese particles. As the outer region has no separate manganese particles hence no iron particle was observed as well. The iron particle was supposed to sink towards the bottom, because of the difference in density, tough the presence of small amount of iron particle in middle region was mostly because of higher viscosity due to presence of solid MnO particles in the slag phase. The good contact of metal droplets with solid MnO particles may indicate low interfacial energies between them that causes not detachment of metal droplets. Hence, we may conclude that the separation of tiny iron particles from the slag is dependent on the dissolution of solid MnO particles into the molten slag phase and hence the loss of the MnO/iron interfacial area.

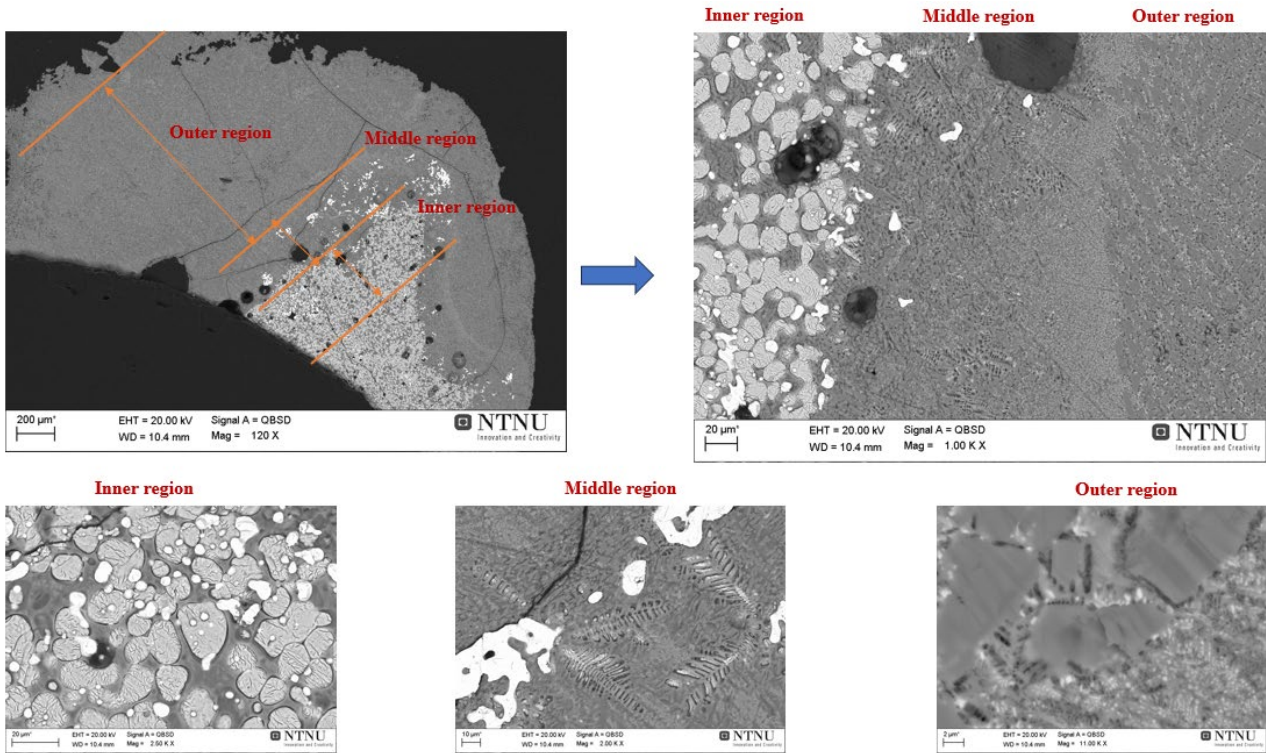


Figure 5: Microstructure of test sample T2 showing different zones of transformation.

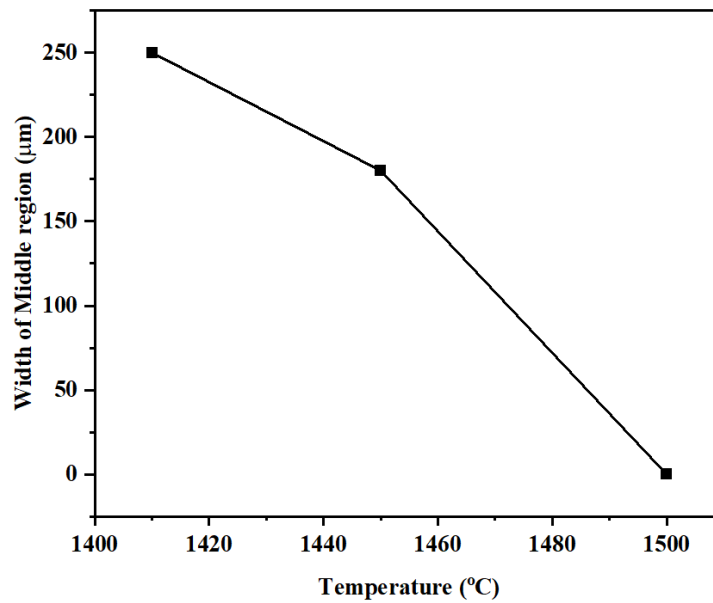


Figure 6: Change in width of partially transformed zone (middle region), with temperature.

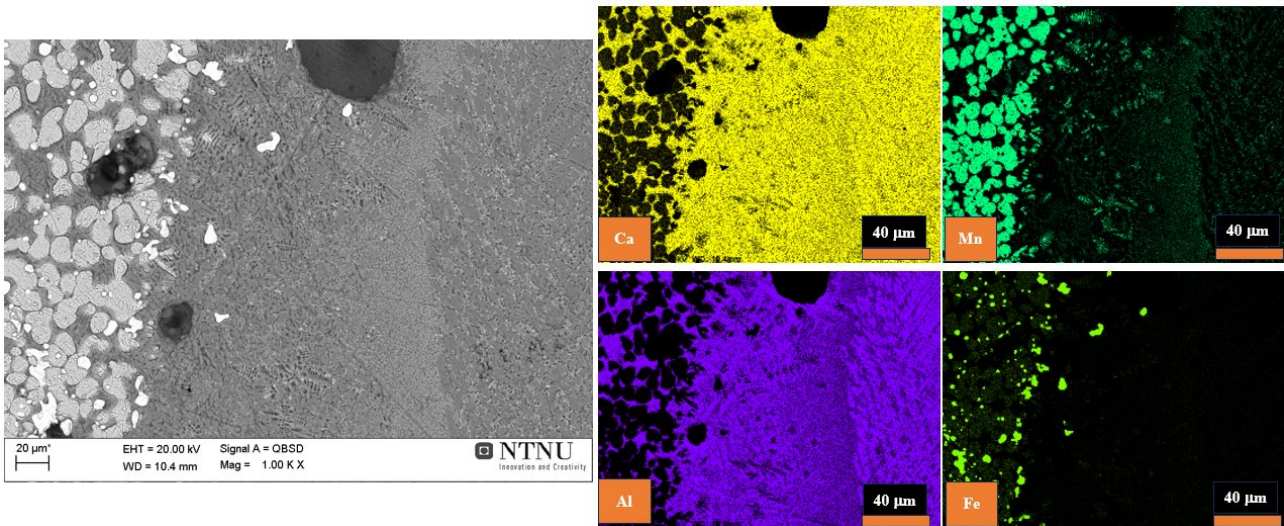


Figure 7: Elemental X-ray mapping image of sample T2 showing the distribution of the main elements.

For the test sample T3, the phases were completely evolved and there was no demarcation of regions as was observed in other samples (T1 & T2). This shows that the melting and the phase formation was completed at 1525 o C. The cross-sectional image of the sample shows a large single metal droplet at the bottom of the melted sample Figure 8, which also signifies complete melting and homogenization of the molten bath. Two distinct phases were observed in the slag, a darker phase consisting of alumina and calcia, in the matrix of a brighter phase consisting of manganese, alumina and calcia. Figure 9 and Table 3 shows the difference in the chemical compositions of these two phases in higher magnification with small area analysis. The darker phase had a  $\text{CaO}/\text{Al}_2\text{O}_3$  mass ratio close to 0.3, which is like that in  $\text{CaO} \cdot 2\text{Al}_2\text{O}_3$  phase. While the  $\text{CaO}/\text{Al}_2\text{O}_3$  mass ratio in case of brighter phase was close to 0.5, which is like that in  $\text{CaO} \cdot \text{Al}_2\text{O}_3$  phase. Hence, it can be very well said that the darker phases were  $\text{CaO} \cdot 2\text{Al}_2\text{O}_3$ , while the brighter ones were  $\text{CaO} \cdot \text{Al}_2\text{O}_3$ .

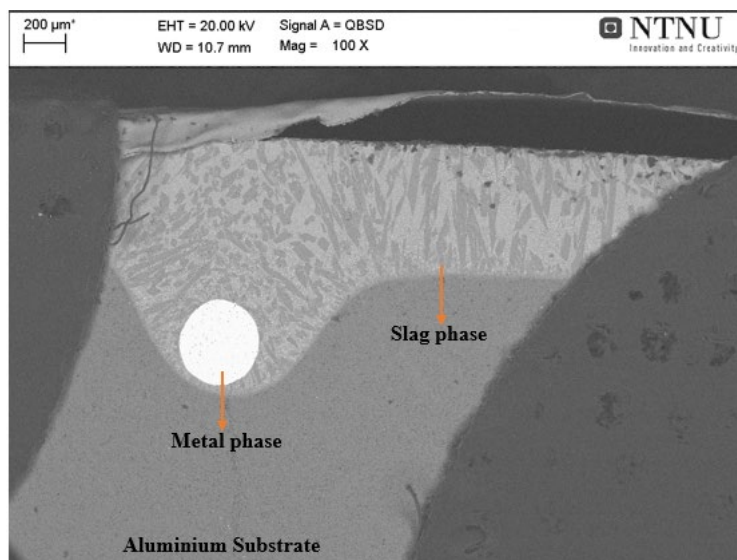


Figure 8: Cross section image of test T3 sample showing metal and slag phase.

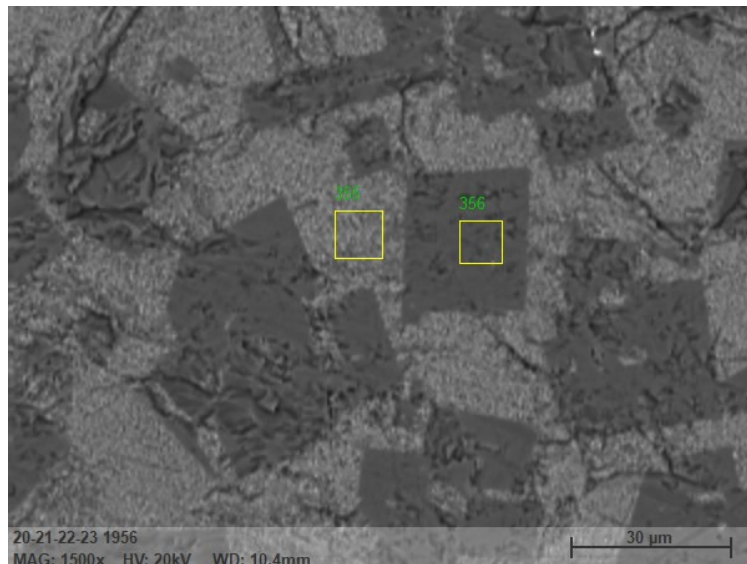


Figure 9: SEM image showing two distinct phases in test T3.

Table 3: EDS result of darker and brighter phases formed in the slag of test T3.

Points/Elements	MnO	CaO	Al <sub>2</sub> O <sub>3</sub>	SiO <sub>2</sub>	MgO
355	19.40	29.7	43.33	3.65	2.314
356	1.53	24.55	73.39	-	-

### 3.3. Probable mechanism

Figure 10 shows the probable mechanism of the melting and dissolution of lime and pre-reduced manganese ore on alumina substrate.

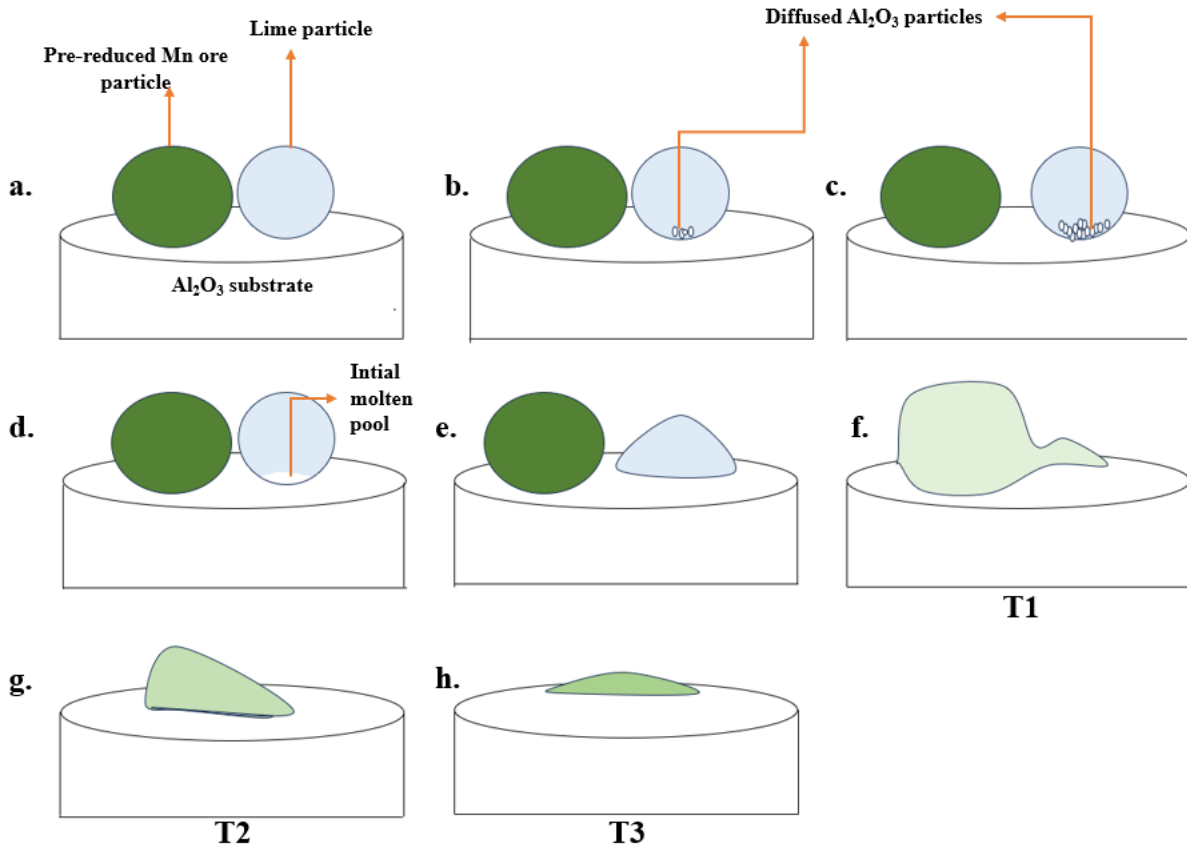
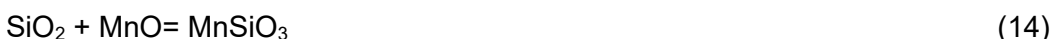


Figure 10: Mechanism of Lime and pre-reduced manganese ore and Alumina substrate interaction.

As the temperature increases, more and more alumina particle from alumina substrate diffuses into the lime particle, which is obvious as diffusion is highly dependent on temperature Figure 11 (b&c). The diffusion of alumina particle would have been significantly easier, as the lime particles were highly porous. However, we may expect that the CaO and adjacent oxides in the lime such as MgO and  $\text{Al}_2\text{O}_3$  and  $\text{SiO}_2$  (Table 2) may yield some early slaggy phases formation in the lime particle, and the free surfaces of the particle and hence the lime/substrate interface. The slow increase in alumina concentration into the lime particle near the interface causes the CaO/ $\text{Al}_2\text{O}_3$  ratio to decrease to lower ratios and eventually to 1, which reflects the eutectic point in CaO- $\text{Al}_2\text{O}_3$  phase diagram Figure 11, marked by arrow. It is at this point that the molten pool starts to form Figure 11d, which explains why the melting of lime particle was observed at 1360 °C, much lower than the theoretical melting point of 2572 °C. Once, the molten pool is formed, the further mechanism is a combination of diffusion and dissolution of lime and alumina into the molten pool. The further melting occurs rapidly and within a narrow temperature zone, because of the combined effect. The concentration of alumina in lime increases rapidly with time and temperature, Eqs. 11-13 show decreasing CaO/ $\text{Al}_2\text{O}_3$  mass ratio from 1.66 to 0.2.



Once the lime is completely molten and spread over the substrate more it touches the solid pre-reduced manganese ore particle, and it covers the particle very rapidly, in a fraction of second, so that a single molten pool is seen while there is an increase in temperature as shown in Figure 11(f-h). The interaction of pre-reduced manganese ore particle with CaO and  $\text{Al}_2\text{O}_3$  starts the slagging reactions with Mn oxide contribution via Eqs. 14 & 15 and the mass transport of MnO to the slag occurs simultaneously via Eq.16, which is solid MnO dissolution into the adjacent molten slag.



MnO (s) = MnO

(16)

At the beginning of the interaction two distinct humps were observed, which slowly reduces to single molten pool at around 1525 °C, marking the end of the reaction. Throughout the reaction the concentration of alumina increases and follows the path marked by arrow on the CaO-Al<sub>2</sub>O<sub>3</sub> phase diagram Figure 11. Upon cooling the phases formed during T1, T2 and T3 is marked on the phase diagram plot with arrow. The melting point increases with increase in Al<sub>2</sub>O<sub>3</sub> content, and the melting point from the phase diagram seems higher than the original melting point during experiment, this is mainly because of impurity such as silica, which is present in the pre-reduced ore. The marked phases are like that observed using SEM analysis discussed earlier.

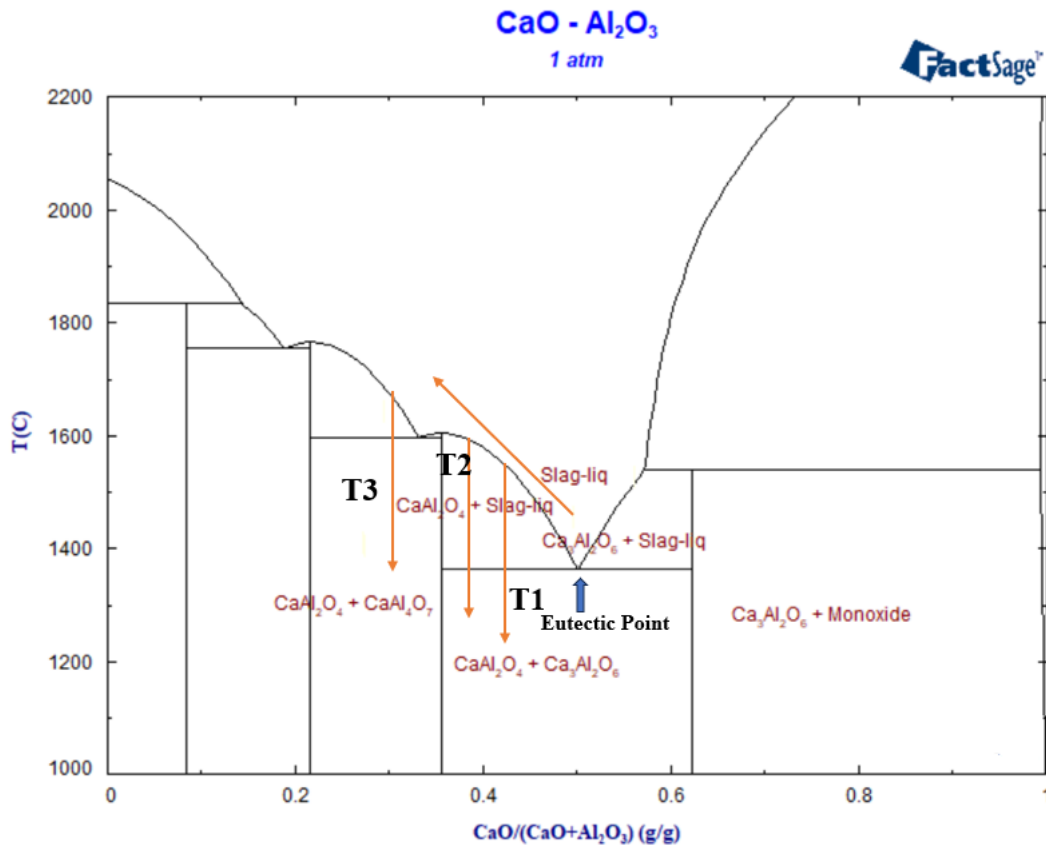


Figure 11: CaO-Al<sub>2</sub>O<sub>3</sub> phase diagram, showing possible phases formed during T1, T2 and T3

#### 4. CONCLUSION

The interaction of lime particles with pre-reduced manganese ore particles on alumina substrate was studied using sessile drop approach. The main conclusions are summarized as follows:

It was found that there is a significant drop in the melting point of lime (theoretically 2572 °C) due to the presence of impurities and adjacent alumina substrate to temperature of 1380 °C

It is proposed that CaO and Al<sub>2</sub>O<sub>3</sub> interact at their contact and the two solids yield a molten interfacial phase that facilitates the rapid melting of CaO particle.

The molten slag and solid Mn ore particle getting united rapidly in the moment the molten slag touches the ore particle. Melting is continued via the dissolution of MnO in the ore into the adjacent molten slag.

The melting or the dissolution rate of Mn ore into the slag is depending on the applied temperature, not complete melting at around 1410 °C, while complete melting at around 1525 °C occurred within 2 minutes.

The separation of molten metal (iron) drops from the pre-reduced ore or slag during the smelting process is depending on the rate and extent of the dissolution of MnO solid particles to the bulk slag, when the solid oxide disappears, the metal is completely separated.

## 5. ACKNOWLEDGEMENT.

The authors would like to thank NTNU for providing the resources and supporting the research work. The authors would also thank all the supporting staff at NTNU. Special thanks to EU council for HalMan project, of which this is a part of.

## 5. REFERENCES

- [1] M. Tangstad and S. E. Olsen, "The Ferromanganese process- Material and Energy Balance," *INFACON 7*, pp. 621–630, 1995.
- [2] "Office of Air Quality Planning and Standards. Background Report-AP-42 Section 12.4 Ferroalloy Production; Report Number: OAQPS/TSD/EIB; Research Triangle Park, NC 27711; U.S. Environmental Protection Agency." Washington, DC, USA, 1992.
- [3] B. Monsen, M. Tangstad, I. Solheim, M. Syvertsen, R. Ishak, and H. Midtgaard, "CHARCOAL FOR MANGANESE ALLOY PRODUCTION," pp. 297–310, 2007.
- [4] N. Haque and T. Norgate, "Estimation of greenhouse gas emissions from ferroalloy production using life cycle assessment with particular reference to Australia," *J. Clean. Prod.*, vol. 39, pp. 220–230, Jan. 2013, doi: 10.1016/j.jclepro.2012.08.010.
- [5] L. A. Westfall, J. Davourie, M. Ali, and D. McGough, "Cradle-to-gate life cycle assessment of global manganese alloy production," *Int. J. Life Cycle Assess.*, vol. 21, no. 11, pp. 1573–1579, Nov. 2016, doi: 10.1007/s11367-015-0995-3.
- [6] Olsen, S.E.; Monsen, B.E.; Lindstad, T, "CO<sub>2</sub> Emissions from the Production of Manganese and Chromium Alloys in Norway," *Proc. 56th Electr. Furn. Conf. New Orleans USA*, pp. 363–369, Nov. 1998.
- [7] Schmidt, G. A., Ruedy, R. A., Miller, R. L., and Lacs, A. A, "Attribution of the present-day total greenhouse effect," *J. Geophys. Res.*, vol. 115, no. D20106, 2010, doi: doi: 10.1029/2010JD014287.
- [8] A. Costello *et al.*, "Managing the health effects of climate change," *The Lancet*, vol. 373, no. 9676, pp. 1693–1733, May 2009, doi: 10.1016/S0140-6736(09)60935-1.
- [9] C. Mora *et al.*, "Global risk of deadly heat," *Nat. Clim. Change*, vol. 7, no. 7, pp. 501–506, Jul. 2017, doi: 10.1038/nclimate3322.
- [10] J. Davies *et al.*, "The Use of Hydrogen as a Potential Reductant in the Chromite Smelting Industry," *Minerals*, vol. 12, no. 5, p. 534, Apr. 2022, doi: 10.3390/min12050534.
- [11] A. Heidari, N. Niknahad, M. Iljana, and T. Fabritius, "A Review on the Kinetics of Iron Ore Reduction by Hydrogen," *Materials*, vol. 14, no. 24, p. 7540, Dec. 2021, doi: 10.3390/ma14247540.
- [12] H. E. Barner and C. L. Mantell, "Kinetics of Hydrogen Reduction of Manganese Dioxide," *Ind. Eng. Chem. Process Des. Dev.*, vol. 7, no. 2, pp. 285–294, Apr. 1968, doi: 10.1021/i260026a023.
- [13] J. Safarian, "A Sustainable Process to Produce Manganese and Its Alloys through Hydrogen and Aluminothermic Reduction," *Processes*, vol. 10, no. 1, p. 27, Dec. 2021, doi: 10.3390/pr10010027.
- [14] F. I. Azof, L. Kolbeinsen, and J. Safarian, "The Leachability of Calcium Aluminate Phases in Slags for the Extraction of Alumina".